Desalination and Water Treatment
www.deswater.com
doi: 10.1080/19443994.2014.936516

56 (2015) 181–193
September

Taylor & Francis
Taylor & Francis Group

Photocatalytic treatment of wastewater containing Rhodamine B dye via Nb_2O_5 nanoparticles: effect of operational key parameters

Fatemeh Hashemzadeh[a], Rahmatollah Rahimi[a,*], Ali Gaffarinejad[a], Vahideh Jalalat[a], Siamak Safapour[b]

[a]*Department of Chemistry, Iran University of Science and Technology, Tehran 16846-13114, Iran, Tel. +982177240290; Fax: +98217791204; emails: Fa_hashemzadeh33@iust.ac.ir (F. Hashemzadeh), Rahimi_Rah@iust.ac.ir (R. Rahimi), Ghaffarinejad@iust.ac.ir (A. Gaffarinejad), jalalat_vahideh@yahoo.com (V. Jalalat)*
[b]*Faculty of Carpet, Tabriz Islamic Art University, Tabriz, Iran, Tel. +984115412140; email: s_safapour@tabriziau.ac.ir*

Received 19 October 2013; Accepted 14 June 2014

ABSTRACT

Heterogeneous photocatalysis has proved to be a useful tool for the degradation of water pollutants over the past 30 years. In this work, the photocatalytic decolorization of Rhodamine B (RhB) dye as a model compound has been studied by using nano-sized Nb_2O_5 semiconductor as a photocatalyst. Structural and textural features of the Nb_2O_5 sample were characterized by X-ray diffraction, scanning electron microscope, UV–vis DRS, and Brunauer–Emmett–Teller techniques. As a result, the orthorhombic Nb_2O_5 particles displayed nearly spherical shape with the average crystalline size and the band gap energy of 43.7 nm and 2.9 eV, respectively. Different parameters of decolorization reaction like dye concentration, catalyst amount, pH, and H_2O_2 concentration have been studied. The optimum conditions for the photo treatment of the dye were initial concentration 10 mg L^{-1} of dye, catalyst concentration 0.5 g L^{-1}, and pH 4. The optimum value of H_2O_2 concentration for the conditions used in this study was 700 mg L^{-1}. Moreover, the efficiency of photo-Fenton process either alone or in conjunction with Nb_2O_5 and a dark-Fenton process as a control experiment were evaluated. The combination of photo-Fenton and Nb_2O_5 catalysts was found to be most effective for the treatment of such type of wastewaters.

Keywords: Heterogeneous photocatalysis; Photo treatment; Rhodamine B; Nb_2O_5 semiconductor; Dark-Fenton; Photo-Fenton

1. Introduction

Colored compounds comprising pigments and dyes are used widely in textile, plastic, food, dyeing, paper, printing, pharmaceutical, and cosmetic industries. These dyes color the water and make penetration of sunlight to the lower layers impossible and hence affecting aquatic life. Rhodamine B (RhB) is one of the famous dyes and is a highly water-soluble, basic red dye of the xanthene class. It is widely used as a dye laser substance and in textiles industry owing to its high stability. Thereby, the removal of this toxic dye is considered one of the important challenges in the recent years using simple and low-cost processes [1–4]. Due to the high concentration of organics in the effluents and the higher stability of modern synthetic dye, the conventional biological treatment methods

*Corresponding author.

1944-3994/1944-3986 © 2014 Balaban Desalination Publications. All rights reserved.

are ineffective for the complete color removal and degradation of organics and dyes [5,6]. Other conventional methods of color removal from an aqueous medium include techniques like coagulation, filtration, adsorption by activated carbon, and treatment with ozone [7].

Each method has its own advantages and disadvantages. For example, the use of charcoal is technically easy but has a high waste disposal cost. While in filtration, low-molar-mass dyes can pass through the filter system. Coagulation, using alum, ferric salts, or lime, is a low-cost process. However, the disposal of toxic sludge is a severe drawback in all the above methods. Lastly, the ozone treatment does not require disposal but suffers from high cost.

In order to overcome these drawbacks, the new oxidation technology known as advanced oxidation processes (AOPs), especially heterogeneous photocatalysis, has been reported as the most effective process for the degradation of various organic compounds and dyes [8–11].

In this study, we focused on niobium oxide (Nb_2O_5), which has been useful as a catalyst [12,13]. Nb_2O_5 is an important wide band gap (3.4 eV) semiconductor oxide which has chemical inertness, thermodynamic stability, and low cytotoxicity. It has been widely used in electrochromic devices [14], gas sensors [15], optical filters [16], and also as a candidate material for photocatalysts [17], biomaterials [18], Li ion battery [19], etc.

Nb_2O_5 is found to exist in different polymorphic forms: H-Nb_2O_5 (pseudo-hexagonal), O-Nb_2O_5 (orthorhombic), and M-Nb_2O_5 (monoclinic) [20]. Among these phases, the M-phase is the most thermodynamically stable form, whereas the H-phase is the least stable one and can be readily transformed into the M-phase by heat treatment at a high sintering temperature. Qi et al.[21] synthesized niobium oxide nanofibers by sol–gel-based electrospinning technique and evaluated photocatalytic activities of the obtained nanofibers depending on the degradation of methyl orange. Ge et al.[22] demonstrated that carbon-modified Nb_2O_5 nanostructures are effective visible light photocatalyst on degradation of RhB.

Degradation of dyes employing the Fenton reagent as another AOP process provides a newer method for the treatment of wastewater containing dye effluents [23]. The Fenton-like processes are used as a powerful source of hydroxyl radicals from H_2O_2 in the presence of transitional metal cations, such as iron, $Fe^{2+}/Fe^{3+}/H_2O_2$, to decompose many organic compounds including dyes. The Fenton reagent as an established reagent for the degradation of dyes suffers the main disadvantage, that is, the reaction ceases after complete consumption of Fe^{2+}, whereas, in the photo-Fenton reaction, Fe^{2+} are regenerated from Fe^{3+} with the additional requirement of light. This makes the process cyclic in nature and the photochemical degradation proceeds smoothly.

Devi et al. [24] investigated the photo degradation of Amaranth (AR) dye by advanced photo-Fenton process and the influence of various reaction parameters such as various aromatic derivatives on the rate of degradation. Soon and Hameed [25] investigated the heterogeneous catalytic treatment of synthetic dyes in aqueous media using Fenton and photo-assisted Fenton processes.

In the present study, photocatalytic decolorization of RhB (as the model dye compound) was used to demonstrate the performance and behaviors of Nb_2O_5 nanoparticles under various conditions. The effects of various key parameters such as catalyst loading, initial dye concentration, pH, and hydrogen peroxide concentration (H_2O_2) were investigated on the photocatalytic treatment of RhB under irradiation of UV light. Moreover, the efficiency of photo-Fenton reaction to decolorize the solution either alone or in conjunction with Nb_2O_5 photocatalyst was evaluated. The effect of Fe^{2+} ion concentration on the decolorization efficiency of RhB in photo-Fenton process was also investigated.

2. Experimental

2.1. Materials and chemicals

Rhodamine B (RhB) was purchased from Sigma–Aldrich. This model dye is highly water soluble (solubility in water = 34 g L^{-1} at 20°C and $pK_a = 3.7$). Fig. 1 presents the molecular structure, chemical properties, and UV–vis absorption spectra of aqueous solutions of RhB.

Niobium pentoxide nanoparticles (molecular formula: Nb_2O_5 (L375968); crystallographic phase: Orthorhombic (T-phase); specific surface area~10 $m^2 g^{-1}$; crystallite size: 43.7 nm; band gap (B.G): 2.9 eV; analytical grade), hydrochloric acid (HCl, 37%), sodium hydroxide (NaOH, 99%), hydrogen peroxide solution (30% w/w), and ferrous sulfate heptahydrate ($FeSO_4{\cdot}7H_2O$) were obtained from Merck company. Deionized water obtained with ion exchanger resins was used for the preparation of different aqueous solutions.

2.2. Apparatus

The self-made photocatalytic system used in this study is shown in Fig. 2 that consists of three parts: a

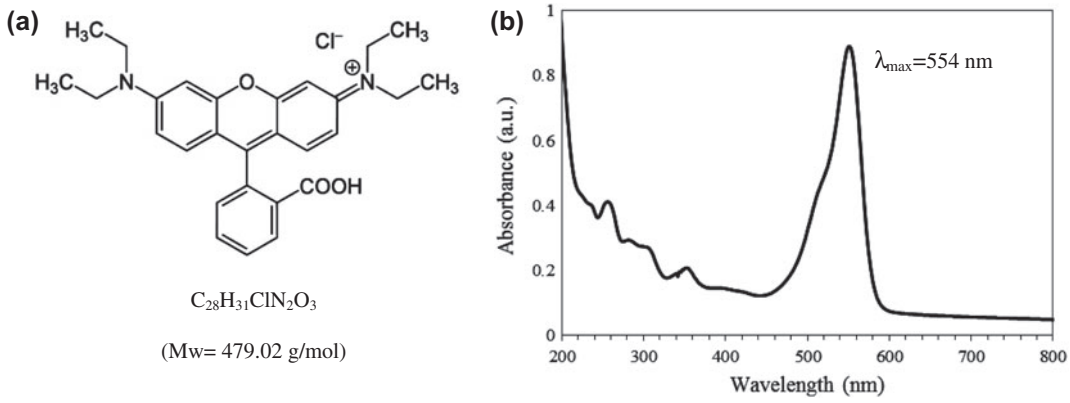

Fig. 1. Chemical structure of Rhodamine B (RhB) (a) and UV–vis absorption spectra of aqueous solutions of Rhodamine B (b).

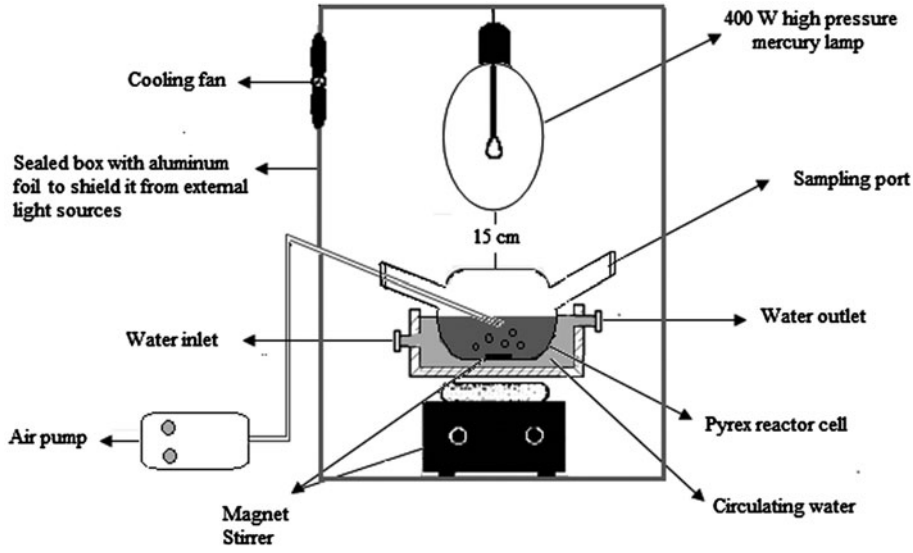

Fig. 2. Schematic diagram of the self-made photocatalytic setup.

sealed box with an aluminum foil to shield it from external light sources; a Pyrex reactor cell of 12 cm height and effective volume of 200 mL with two faucets; and a 400 W high-pressure Hg lamp (OSRAM HQL (MBF-U), made in EC 3738) with a major emission at about 365 nm, which was positioned on top of the reactor cell as shown in Fig. 2.

The distance from the lamp to the top of the reactor was 15 cm. An air pump provides compressed air to ensure a constant supply of oxygen to the reaction volume and a complete mixing of solution and photocatalysts during the photoreaction. The reaction mixture was also under continuous stirring throughout the experiment.

In all experiments, the reaction temperature was kept at 25 ± 2℃ using a cooling fan and circulating water.

2.3. Experimental

2.3.1. Characterization of Nb_2O_5 photocatalyst

Powder X-ray diffraction (XRD) method was used for crystal phase identification and the estimation of crystallite size. XRD pattern was obtained on a Philips diffractometer (PW1800) using monochromatized Cu Kα radiation ($\lambda = 0.15406$ nm) at 40 kV and 30 mA. Diffraction patterns were collected from 4° to 90° at a speed of 10° min^{-1}. The morphology was also characterized using scanning electron microscope (SEM) VEGASEM, II SBU-VG5200879IR. The Brunauer–Emmett–Teller (BET) surface areas of the Nb_2O_5 sample were measured by nitrogen adsorption at 77 K using a Micromeritics BET (ASAP 2020) adsorption analyzer. UV–vis diffuse reflectance spectra were recorded on a Shimadzu (Mini1240) spectrophotometer.

2.3.2. Photocatalytic activity test

The photocatalytic activity of Nb_2O_5 nanoparticles under UV irradiation was evaluated by using RhB as the model substrate. In a typical process, 0.025 g catalyst was suspended in 50 mL RhB aqueous solution (10 mg L^{-1}, pH value: 5 (natural pH)) under ultrasonication for 3 min in a Pyrex reactor cell. The suspension was stirred in the dark for about 60 min before the light was turned on. The suspension was sampled from the reactor cell using a glass syringe at timed intervals during reaction and centrifuged immediately for separation of the suspended solids. For comparison, experimental runs with irradiation but without the catalyst and the one with catalyst but without the use of irradiation were also performed to demonstrate the decolorization efficiency contributed to photolysis and adsorption process, respectively . To probe the dependence of the decolorization efficiency of RhB upon various influencing key factors, a series of experiments were carried out at different photocatalytic conditions.

The additional amount of nano-sized Nb_2O_5 powder was varied from 0.1 to 2 g L^{-1}. Initial organic content (5–25 mg L^{-1}), solution acidity (pH 2–11), and H_2O_2 concentration (100–1,000 mg L^{-1}), as well as the effect of photo-Fenton reaction either alone with varying Fe^{2+} concentration or in conjunction with Nb_2O_5 photocatalyst on the efficiency of the reaction, were also investigated. The original pH of the aqueous solution was about 5. For evaluation of other values of pH, 0.01 M HCl or 0.01 M NaOH was added prior to any experimental run. The aerating rate of air and reacting temperature were controlled at 30 mL min^{-1} and 25˚C, respectively.

In order to develop optimized pH for the decolorization of RhB, the point of zero charge (PZC) pH of Nb_2O_5 photocatalyst was measured by the so-called pH drift method [26]. At $pHs > pH_{pzc}$, the total surface of the Nb_2O_5 catalyst is negatively charged [27], while at $pHs < pH_{pzc}$, the surface has a net positive charge.

2.4. Analysis of liquid samples

After the desired reaction time, 5 mL of liquid sample was collected from the reaction cell and centrifuged at 14,000 rpm to settle down the catalysts using a Nüve centrifuge (model NF800). Evaluation of the photocatalytic activities of the photocatalyst was conducted by recording the variations of the absorption band maximum ($\lambda_{max} = 554$ nm) as a function of irradiation time through a UV–vis spectrophotometer (Shimadzu UV-1700).

The decolorization efficiency of Rhodamine B was calculated by Eq. (1):

$$\text{Decolorization efficiency}\,(\%) = \frac{C_0 - C_t}{C_0} \times 100 \qquad (1)$$

where C_0 is the initial concentration of RhB solution which reached absorbency balance and C_t is the concentration of the dye solution at the irradiation time (t).

3. Results and discussion

3.1. Microstructure characterization

The XRD result taken from the Nb_2O_5 powder is displayed in Fig. 3. The XRD measurement showed that the Nb_2O_5 sample existed in the orthorhombic structure because only the characteristic peaks of the orthorhombic phase (space group: Pbam (55), JCPDS No. 30–0873) containing $2\theta = 28.23^\circ$, 22.49°, 36.43°, and 28.82° diffraction lines were observed. The average crystallite size of orthorhombic Nb_2O_5 was calculated using Scherrer's equation $D = k\lambda/\beta\cos\theta$, where D is the crystallite size, k is the Scherrer constant ($k = 0.9$ assuming that the particles are spherical), λ is the wavelength of the X-ray radiation (Cu K_α radiation, $\lambda = 0.15406$ nm), β is the line width at half-maximum (obtained after correction for instrumental broadening), and θ is the diffraction peak angle. The crystalline size pertaining to three-intense reflections was determined using the Scherrer equation. The average crystallite size of Nb_2O_5 particles was determined to be 43.7 nm.

The morphology of the orthorhombic Nb_2O_5 sample was also investigated by SEM micrographs. As shown in Fig. 4, Nb_2O_5 consisted of many nearly spherical shaped particles approximately <100 nm in size.

Fig. 5 shows that N_2 adsorption–desorption isotherm of Nb_2O_5 sample exhibits typical type III of IUPAC classification, indicating weak interaction between absorbent and absorbed, which belongs to macroporous material or is mesoporous with irregular porosity. The result of N_2 adsorption–desorption suggested that the BET specific surface area of Nb_2O_5 was 9.8 $m^2 g^{-1}$.

Before the photocatalytic activity characterization, it is also important to study the optical absorption of the Nb_2O_5 sample, because the UV–vis absorption edge is relevant to the energy band of the semiconductor catalyst. The photo absorption performance and the band gaps of the samples are shown in Fig. 6. As shown in the UV–vis spectra, two major absorption

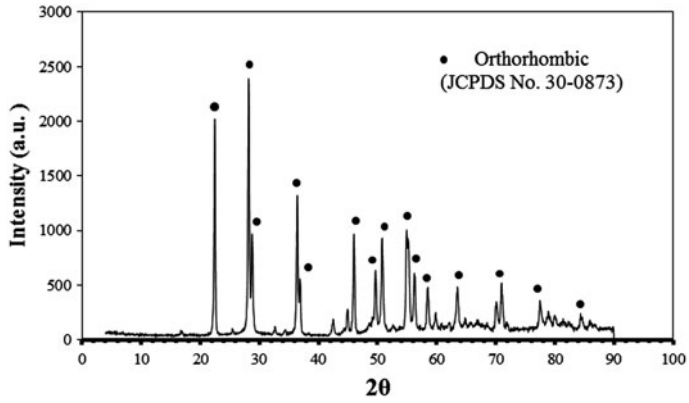

Fig. 3. XRD pattern of niobium oxide sample.

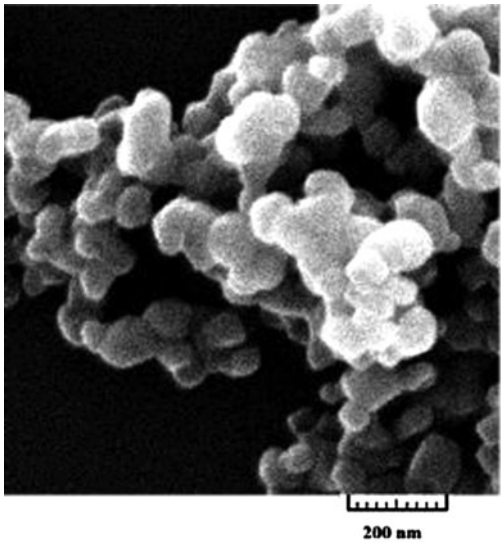

Fig. 4. SEM photograph of Nb_2O_5 sample.

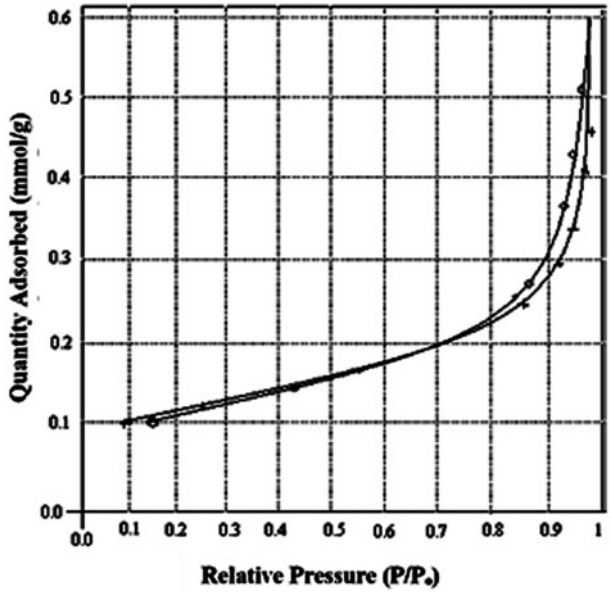

Fig. 5. The N_2 adsorption–desorption isotherm of Nb_2O_5 nanoparticles.

bands for Nb_2O_5 powder with maxima appear at about 220 and 308 nm. The absorption band above 300 nm corresponds to the excitonic or interband (valence to conduction bond) transition, while the band at 220 nm is typically associated with NbO bonds, which is unambiguously assigned to the ligand-to-metal charge transfer transition. This charge transfer occurs with electron excitation from oxygen to an unoccupied orbital of the Nb ions surrounded by oxygen [28].

Using the $\alpha = A\ ((h\nu - E_g)^{n/2})/(h\nu)$ equation is more accurate for determination of the semiconductor band gap energy (E_g). Here, α, ν, E_g, and A are absorption coefficient, light frequency, band gap, and a constant, respectively. Among them, n depends on whether the transition is direct ($n = 1$) or indirect ($n = 4$) [29]. The band gap can be estimated by extrapolating the rising linear portion of the $(\alpha h\nu)^{1/2}$ vs. $h\nu$ curve to the abscissa at zero absorption. The band gap energy of orthorhombic Nb_2O_5 was estimated to be 2.9 eV.

3.2. Photocatalytic activity

The decolorization of RhB was performed under different experimental conditions that include: (i) RhB dye solution in the absence of photocatalyst under irradiation of UV light (photolysis); (ii) reaction mixture of RhB dye solution and Nb_2O_5 photocatalyst ($0.5\ g\ L^{-1}$) in the absence of UV light (Adsorption); and (iii) reaction mixture of RhB dye solution and Nb_2O_5 photocatalyst ($0.5\ g\ L^{-1}$) under irradiation of

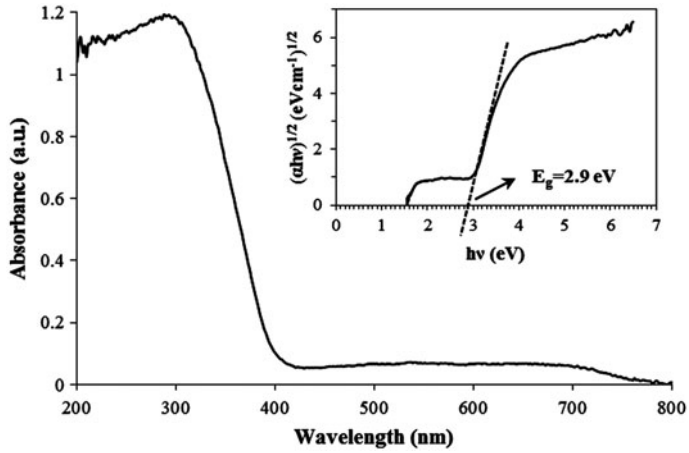

Fig. 6. DRS UV–vis absorption spectra and the plots for band gap energy (E_g) measurement (inset) of Nb_2O_5 photocatalyst.

UV light (photocatalysis), and the results are shown in Fig. 7.

Control experiments (without UV and photocatalyst) revealed no significant decolorization of RhB. However, under UV irradiation, approximately 6% decolorization of RhB was achieved within 120 min of irradiation time compared to 2% achieved under adsorption without UV light. The decolorization percent rapidly rises to 51% after 120 min of treatment when Nb_2O_5 powder is added to the RhB solution as shown in Fig. 7.

Fig. 7 implies that the photocatalytic decolorization of RhB obeys the first-order decay kinetics according to Eq. (2):

$$C = C_0 \exp(-kt) \quad \text{or} \quad \ln\left(\frac{C}{C_0}\right) = -kt \tag{2}$$

where C_0 is the initial concentration of RhB (mole L^{-1}), C is the concentration of the dye at various interval times (mole L^{-1}), t is the illumination time (min), and k is the reaction rate constant. Plotting $-\ln(C/C_0)$ vs. t gives the apparent rate constant for decolorization of RhB from the slope of curve-fitting line and the intercept is equal to zero. Meanwhile, the linear relationship between $-\ln(C/C_0)$ and t indicates that the photocatalytic decolorization reaction also follows the pseudo first-order reaction; the apparent rate constants were calculated to be 4×10^{-5}, 1.0×10^{-3}, and 5×10^{-3} min^{-1} for Nb_2O_5 photocatalyst only (adsorption) (i), photolysis only (ii), and photocatalysis (iii), respectively.

Niobium pentoxide is a best candidate for clean photocatalytic processes that mineralize several dyes into nontoxic species. Once niobium pentoxide is

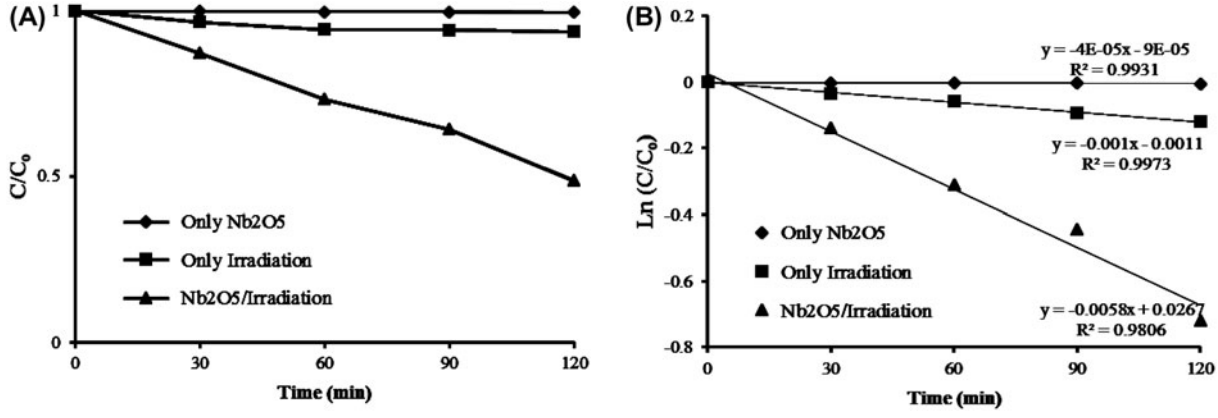

Fig. 7. Decolorization of RhB dye (10 mgL^{-1}) during the adsorption (only Nb_2O_5), photolysis (only Irradiation) and photocatalysis (Nb_2O_5/Irradiation) experiments (A); the kinetics of the three mentioned experiments (B).

illuminated by light with energy higher than its band gap, the electrons in the lower valence band absorb a definite amount of energy and jump to the higher conduction band that leads to the formation of positive hole and negative electron, which migrate to the catalyst surface as active charge carriers. The positive hole can react with water or hydroxyl ions, thus producing hydroxyl radicals, and electron in the conduction band (e_{CB}^-) on the catalyst surface can reduce molecular oxygen to superoxide anion. Hydroxyl ($HO^\bullet$), hydrogen peroxides ($HO_2^\bullet$), and superoxide ($\bullet O_2^-$) radicals are considered the reactive species that will oxidize the organic compounds adsorbed on the oxide surface [30,31]. These generated radicals are the responsible active species for complete mineralization of the hazardous dyes. Various parameters must be achieved to maximize the photocatalytic activity of niobia for decolorization of RhB as the catalyst amount, initial dye concentration, pH, concentration of hydrogen peroxide (H_2O_2), concentration of Fe^{2+} in the presence of H_2O_2, and $Fe^{2+}/H_2O_2/Nb_2O_5$ system.

3.2.1. The effect of initial concentration of RhB

It is important from an application point of view to study the dependence of decolorization efficiency on the initial concentration of dye in wastewater. Therefore, the effect of initial RhB concentration on the photocatalytic RhB decolorization process was investigated by treating different initial concentrations of RhB: 5, 10, 15, 20, and 25 mg L^{-1} at pH 5 (natural pH) and with catalyst concentration of 0.5 g L^{-1}. It is apparent from the results in Fig. 8 that the decolorization efficiency decreased with increasing RhB concentration from 5 to 25 mg L^{-1}. The percentage of decolorization was 61% in the case of 5 mg L^{-1}, and 10% for 25 mg L^{-1}, respectively, at the end of 2 h.

This can be explained by the following causes: assuming that most of the reactions take place at the surface of the photocatalyst, with increasing initial concentration of RhB and corresponding intermediates, the RhB decolorization has been limited by the available surface area. Moreover, due to this, only fewer photons reach the surface of the photocatalyst. This results in the decrease in concentration of $^\bullet OH$ and $O_2^{\bullet-}$ radicals, thereby decreasing the photocatalytic activity.

3.2.2. Effect of catalyst amount

From an economical point of view, in any decolorization process the catalyst concentration is considered as one of the most important parameters that should be investigated. The effect of catalyst amount on the photocatalytic decolorization process of RhB was investigated using different amounts of Nb_2O_5 catalyst varying from 0.1 to 2 g L^{-1} by keeping all other experimental parameters constant. The optimal concentration of RhB (10 mg L^{-1}) was used in all experiments. Results are presented in Fig. 9.

Within the range of catalyst amounts from 0.1 to 2 g L^{-1}, the observed enhancement in decolorization may be due to an increased number of available adsorption and catalytic sites on the surface of Nb_2O_5 catalyst. A further increase in catalyst concentration, however, may cause an increase in opacity and a light-scattering effect, which will reduce its specific activity by aggregation of Nb_2O_5 particles under high dosage amount. Further, at higher catalyst concentration, it is difficult to maintain a homogeneous suspension due to agglomeration of the particles, which decreases the number of active sites. The results indicate that an optimized catalyst concentration (0.5 g L^{-1}) is necessary for enhancing the decolorization efficiency.

3.2.3. The effect of pH

The solution pH has profound influences on the adsorption and dissociation of the substrate, catalyst surface charge, the oxidation potential of the valence band, and other physicochemical properties of the system [32,33]. Therefore, determining the effects of pH on the RhB decolorization efficiency in the UV/Nb_2O_5 system is extremely difficult. Additionally, pH changes influence the adsorption of RhB molecules onto the Nb_2O_5 surface, which is important in photodecolorization.

3.2.3.1. Measurement of pH_{pzc} of Nb_2O_5 photocatalyst. In order to find out optimal pH for the decolorization of RhB, the PZC of Nb_2O_5 was measured by the so-called pH drift method [26]. At pHs > pH_{pzc}, the total surface of the Nb_2O_5 catalyst is negatively charged [27], while at pHs<pH_{pzc}, the surface has a net positive charge. The determination of the pH_{pzc} of the samples was carried out as follows [34]: 50 mL of 0.01 M NaCl solution was placed in a closed Erlenmeyer flask. The pH was adjusted to a value between 1 and 10 by adding HCl 0.1 M or NaOH 0.1 M solution. Then, 0.05 g of Nb_2O_5 sample was added and the final pH was measured after 48 h under agitation at room temperature. The pH_{pzc} is the point where the curve pH_{final} vs. pH_{inital} crosses the line $pH_{initial} = pH_{final}$.

Fig. 10 shows the "'pH drift"' data, from which the pH_{pzc} of the Nb_2O_5 catalyst can be determined (pH 6.8).

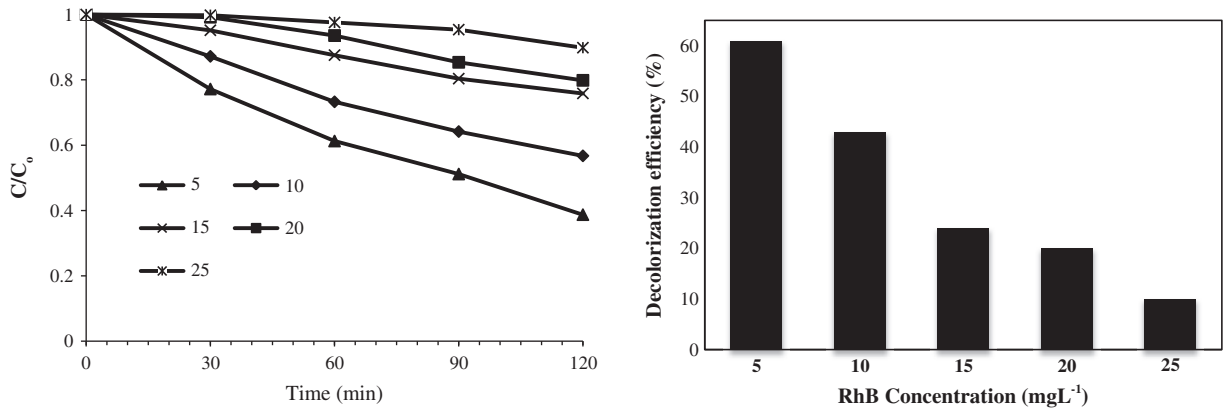

Fig. 8. Photocatalytic decolorization of different concentrations of RhB dye (mg L^{-1}).

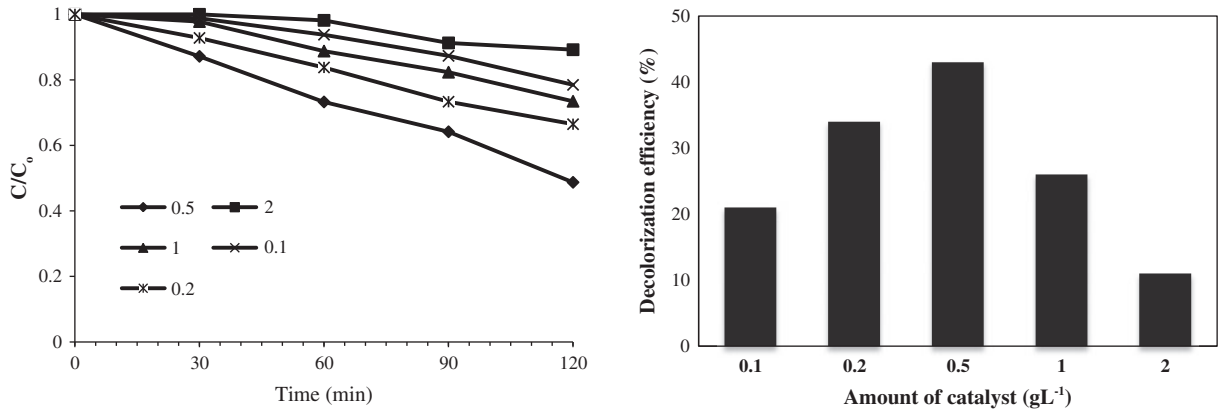

Fig. 9. Effect of catalyst concentration (g L^{-1}) on photocatalytic decolorization of RhB.

This value could change, depending on the nature of dispersion and the difference in catalyst diameter [35–37].

3.2.3.2. The influence of pH on the photocatalytic decolorization of RhB. The influence of pH on the photocatalytic decolorization of RhB was studied in the range of pH between 2 and 11 by keeping the RhB dye concentration (10 mg L^{-1}) and catalyst amount (0.5 g L^{-1}) constant in all reactions and results were shown in Fig. 11. The pH was adjusted by the addition of appropriate amounts of NaOH 0.01 M or HCl 0.01 M solution. The initial pH of the RhB dye solution was 5.

The results shown in Fig. 11 demonstrated that when pH was reduced from 5 (natural pH) to 4, the percentage of decolorization was increased from 43 to 51%. Further decrease in pH to 2, the percentage of decolorization was decreased from 51 to 48%. Similarly, when the pH was increased from 5 to 7, the decolorization percentage was reduced from 43 to

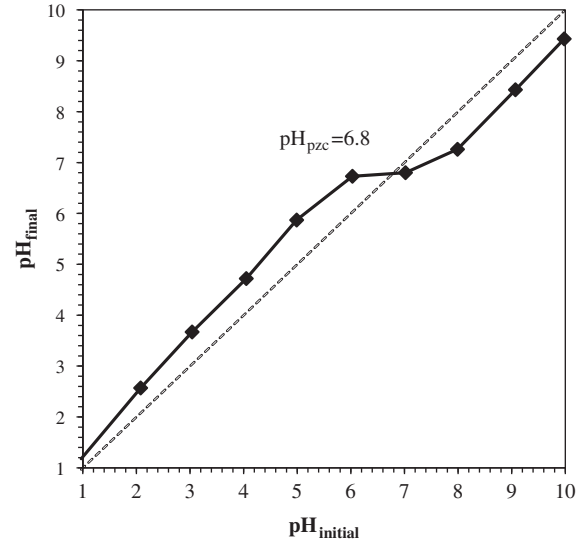

Fig. 10. Determination of pH$_{pzc}$ of Nb_2O_5 catalyst by the pH drift method [26].

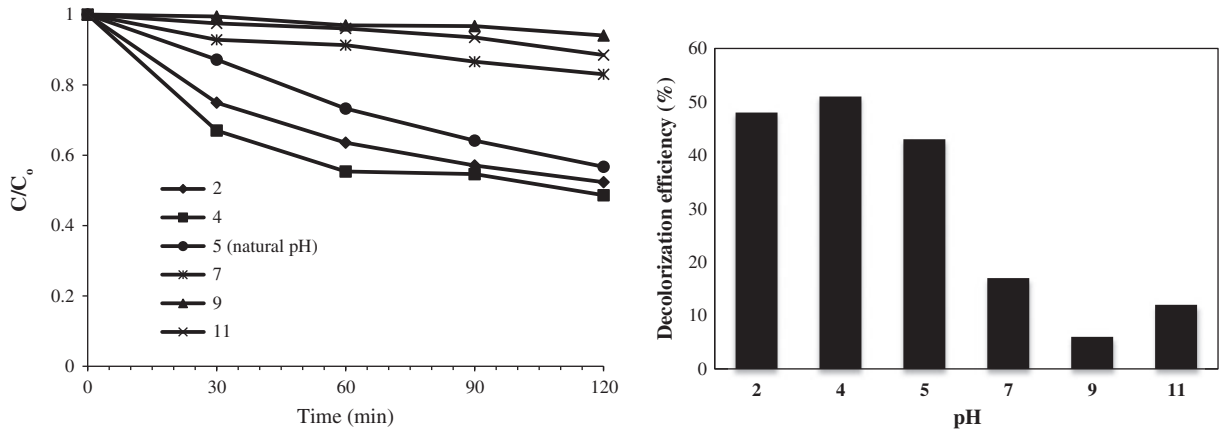

Fig. 11. Effect of pH on photocatalytic decolorization of RhB dye.

17%. It was expected that cationic RhB dye more favorably adsorbed on the negatively charged surface of Nb_2O_5 catalyst in basic medium ($pH > pH_{pzc} = 6.8$) by electrostatic interactions and resulted in high decolorization efficiency, but experimental results demonstrate that decolorization efficiency at acidic medium ($pH < pH_{pzc}$) exceeded the one at basic medium (pHs $> pH_{pzc}$).

Since several reaction mechanisms contribute to dye decolorization, such as hydroxyl radical attack, direct oxidation by positive holes, and direct reduction by electrons, the effect of pH on decolorization efficiency differs from those of photocatalysts and photodecolorization model substrates.

The obviously increased decolorization of RhB with the decreasing of pH value could be interpreted as follows. On the one hand, in acidic condition, more H^+ adsorb onto the photocatalyst and regenerate the catalyst surface sites through timely removal of the intermediate species from the surface [38], thereby improving the decolorization of RhB. Additionally, at pH solution higher than the acid dissociation constant ($pK_a = 3.7$) of RhB, the deprotonation of carboxyl group could easily occur and transform the cationic form of RhB into anionic zwitterionic form [39]. Due to this, dye adsorption on the surface of the catalyst at pH4 exceeded the one at pH5 and decolorization percentage of dye also increased (maximum 51%). Further decrease in pH (pH2) resulted in the decrease in decolorization of the dye. This may be due to the electrostatic repulsive force of positively charged RhB molecules ($pH < pK_{a\ (RhB)} = 3.7$) from the surface of the photocatalyst with a positive charge in acidic medium ($pH < pH_{pzc} = 6.8$), thereby decreasing in decolorization efficiency of the dye.

The results indicated that the pH value of the solution was the key factor for dye decolorization and the optimum pH value for decolorization of RhB dye under irradiation of UV light is 4.

3.2.4. Effect of H_2O_2 concentration

The addition of oxidizing species, such as H_2O_2, during photocatalysis often leads to an increase in the rate of photo-oxidation [40,41].

As shown in Eq. (3), the illumination of Nb_2O_5 with UV light generates holes in the valence bands (h^+), and the electrons in the conduction band (e^-). However, the hole-electron recombination limits the use of Nb_2O_5 photocatalysis system in wastewater treatment. Whereas the electrons are consumed during the reaction with oxygen (O_2) to convert it to the superoxide radical ($O_2^{\cdot -}$) (Eq. (5)), the holes can react with hydroxide ion on the Nb_2O_5 surface to form hydroxyl radicals (Eq. (4)). Therefore, the photocatalytic reaction needs sufficient oxygen (O_2) to suppress this recombination process.

$$Nb_2O_5 \xrightarrow{hv} Nb_2O_5(e^-) + Nb_2O_5(h^+) \quad (3)$$

$$h^+ + OH^-_{ads} \rightarrow {}^{\cdot}OH \quad (4)$$

$$e^- + O_2 \rightarrow O_2^{\cdot -} \rightarrow {}^{\cdot}OH \quad (5)$$

H_2O_2 is considered to have double function in the photocatalytic oxidation process. It could act as an alternative electron acceptor to oxygen because

hydrogen peroxide is a better electron acceptor than molecular oxygen, thereby promoting the charge separation (Eq. (6)).

$$e^- + H_2O_2 \rightarrow OH^- + {}^{\cdot}OH \quad (6)$$

Moreover, hydrogen peroxide also produces hydroxyl radicals via photodecomposition and it inhibits the e− and h + recombination according to the following equations [42,43].

$$H_2O_2 + hv \rightarrow 2{}^{\cdot}OH \quad (7)$$

$$H_2O_2 + O_2^{\cdot -} \rightarrow {}^{\cdot}OH + OH^- + O_2 \quad (8)$$

The catalytic oxidation runs for different H_2O_2 concentrations were carried out using the following operational conditions: Initial pH of 5, catalyst amount of 0.5 g L^{-1}, initial concentration of RhB of 10 mg L^{-1}, H_2O_2 concentration ranging from 100 to 1,000 mg L^{-1}. It was found that the decolorization percent of RhB increased when H_2O_2 concentration was increased from 100 to 700 mg L^{-1} but at higher levels, there was a drop in the decolorization percent (Fig. 12).

The percentage decolorization of RhB dye without addition of H_2O_2 was 43% and after addition of 100, 300, 500, and 700 mg L^{-1} of H_2O_2, it reached to 51, 56, 63, and 66%, respectively. When the amount of H_2O_2 was further increased to 900 and 1,000 mg L^{-1}, the percentage decolorization was 55 and 39% respectively, with a drop in the decolorization efficiency after 2 h irradiation of UV light.

The latter effect may be explained in terms of the fact that H_2O_2 scavenges the photo-generated oxidizing species (i.e. valence band holes and hydroxyl radicals) that are responsible for oxidation of dye molecule (Eqs. (9) and (10)).

$$H_2O_2 + {}^{\cdot}OH \rightarrow H_2O + HO_2^{\cdot} \quad (9)$$

$$HO_2^{\cdot} + {}^{\cdot}OH \rightarrow H_2O + O_2 \quad (10)$$

The selection of the optimum value is important from the commercial point of view (due to the cost of H_2O_2). This optimum value, for the conditions used in this study, seems to be 700 mg L^{-1} because initial decolorization efficiency is much higher than that at other concentrations of H_2O_2 (Fig. 12). Solution pH was not affected significantly by H_2O_2 concentration used in the runs.

3.2.5. The effect of photo-Fenton and photo-Fenton/ Nb_2O_5 processes on the decolorization efficiency of RhB

In the Fenton reaction, ferrous salts react with H_2O_2 to produce $^{\bullet}OH$ radical as shown in Eqs. (11–13) [44].

$$Fe^{2+} + H_2O_2 + H^+ \rightarrow Fe^{3+} + {}^{\cdot}OH + H_2O \quad (11)$$

$$Fe^{3+} + H_2O_2 \rightarrow Fe^{2+} + {}^{\cdot}OOH + H^+ \quad (12)$$

$$Fe^{3+} + {}^{\cdot}OOH \rightarrow Fe^{2+} + O_2 + H^+ \quad (13)$$

The hydroxyl free radical thus generated attacks the unsaturated dye molecules and the azo bond (N=N) in the chromogen, thus decolorizing the wastewater.

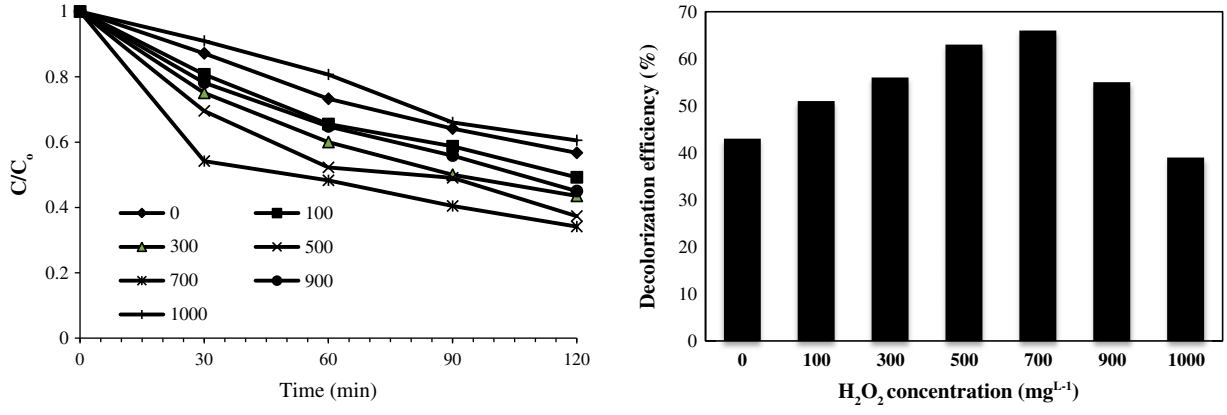

Fig. 12. Effect of H_2O_2 concentration (mg L^{-1}) on photocatalytic decolorization of Rhodamine B.

In the photo-Fenton process, in addition to the above reaction, the formation of hydroxyl radical also occurs by the following reactions (Eqs. (14) and (15)):

$$H_2O_2 + UV \rightarrow {}^{\cdot}OH + {}^{\cdot}OH \quad (14)$$

$$Fe^{3+} + H_2O + UV \rightarrow {}^{\cdot}OH + Fe^{2+} + H^+ \quad (15)$$

The high efficiency of photo-Fenton process is due to the formation of more hydroxyl radical than the other processes. Therefore, the purpose of this section is evaluation of the efficiency of photo-Fenton process to decolorize the RhB solution either alone or in conjunction with Nb_2O_5 photocatalyst. In addition, one control experiment without UV light as dark-Fenton process was conducted to verify the combined effects of Fenton reagent, Nb_2O_5 catalyst, and UV light.

Amount of ferrous ion is one of the main parameters to influence the Fenton and photo-Fenton processes. Therefore, prior to comparative study of photo-Fenton, photo-Fenton/Nb_2O_5, and dark-Fenton processes for decolorizing of RhB solution, a number of experiments were performed to determine the optimum value of Fe^{2+} concentration for effective decolorization of aqueous RhB by photo-Fenton process.

3.2.5.1. Effect of Fe^{2+} concentration on the photo-Fenton decolorization of RhB. The effect of Fe^{2+} concentration (10–90 mg L^{-1}) on the photo-Fenton decolorization of RhB was studied by keeping the initial pH of 5, RhB dye concentration (10 mg L^{-1}), and H_2O_2 concentration (700 mg L^{-1}) constant in all reactions. H_2O_2 is unstable in alkaline solutions, and loses its oxidizing potential. Therefore, the pH of this study focuses on the natural pH of 5. The results presented in Fig. 13 indicated that decolorization efficiency of RhB at 10 mg L^{-1} of Fe^{2+} was 92% within 14 min, whereas 99% decolorization obtained within 2 min at 50 mg L^{-1} of Fe^{2+}. More hydroxyl radicals are produced with the increase in the concentration of Fe^{2+} up to an optimal value, since ferrous ion catalyses H_2O_2 to form hydroxyl radical quickly.

However, a further increase in Fe^{2+} concentration decreased decolorization efficiency. This phenomenon is due to the fact that $HO^{\bullet}$-scavenging reactions became more and more dominant at excessive Fe^{2+} concentrations [45] according to reaction (Eq. (16)):

$$Fe^{2+} + {}^{\cdot}OH \rightarrow Fe^{3+} + OH^- \quad (16)$$

3.2.5.2. The efficiencies of dark-Fenton, photo-Fenton and photo-Fenton/Nb_2O_5 processes on the decolorization of RhB. In the second part of the study, photo-Fenton alone and photo-Fenton in conjunction with Nb_2O_5 photocatalyst and one control experiment without UV light as dark-Fenton processes were compared in terms of RhB decolorization to verify the combined effects of Fenton reagent, Nb_2O_5 catalyst, and UV light.

The experimental results revealed that the RhB dye was most rapidly decolorized by the photo-Fenton/Nb_2O_5 process (100% within 1 min) followed by photo-Fenton (99% within 2 min) and dark-Fenton (76% within 15 min) processes (Fig. 14).

During the application of photo-Fenton/Nb_2O_5 and photo-Fenton treatment, RhB decolorized up to 100 and 99% after only 1 and 2 min treatment, respectively, while it took up to 15 min with the dark-Fenton process to decolorize only 76% of RhB. Hence, photo-Fenton process and photo-Fenton/Nb_2O_5 process are more efficient than dark-Fenton process. The enhancement of

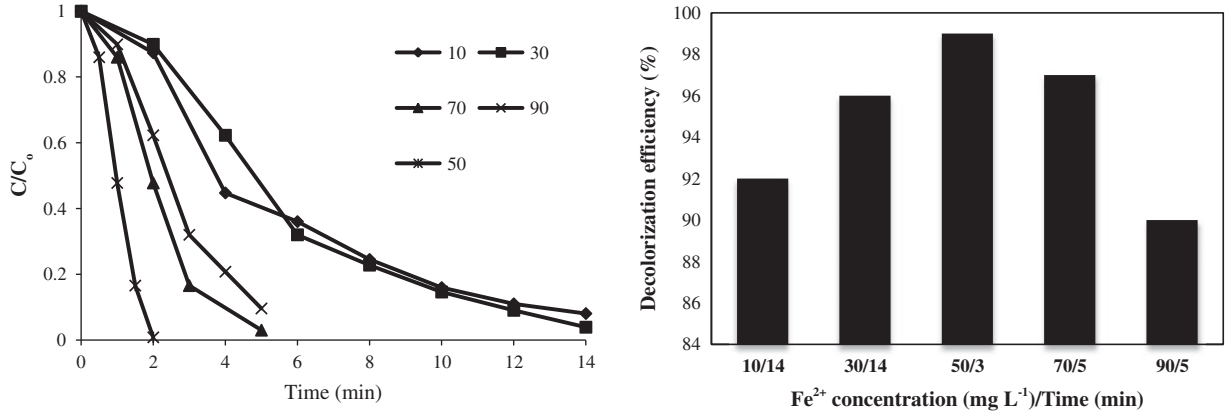

Fig. 13. The effect of Fe^{2+} concentration (mg L^{-1}) on the photo-Fenton decolorization of RhB.

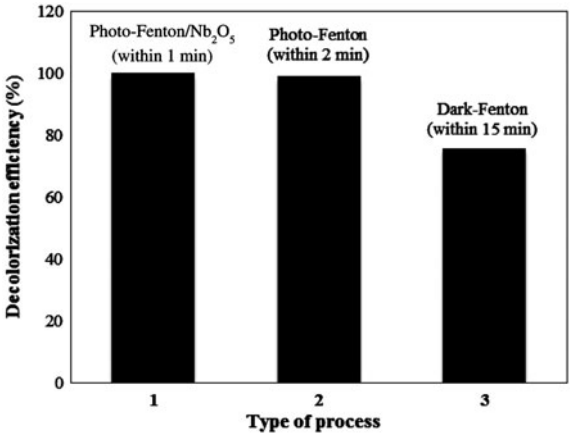

Fig. 14. The decolorization efficiency with required time of photo-Fenton, photo-Fenton/Nb_2O_5, and dark-Fenton processes to decolorize the RhB solution (10 mg L^{-1}).

RhB decolorization efficiency in the photo-Fenton process in conjunction with Nb_2O_5 photocatalyst was most probably caused by the generation of additional HO• according to Eqs. (4, 5, and 11–15).

4. Conclusions

In this research, photocatalytic treatment of Rhodamine B (RhB) dye was studied using Nb_2O_5 nanoparticles as photocatalyst. The effects of operational key parameters such as initial RhB concentration, Nb_2O_5 amount, pH, and H_2O_2 concentration on the decolorization efficiency of RhB were investigated. It was found that the decolorization was suppressed by increasing the initial dye concentration. Experimental results indicate that the decolorization efficiency increased with increasing the Nb_2O_5 concentration up to 0.5 g L^{-1}, beyond which the decolorization efficiency decreased. Higher decolorization efficiencies were obtained at acidic pH values. The addition of H_2O_2 improved the decolorization efficiency up to certain value (700 mg L^{-1}). Moreover, we evaluate the efficiency of photo-Fenton process either alone or in conjunction with Nb_2O_5 photocatalyst and a dark-Fenton process as a control experiment to decolorize the RhB solution. The experimental results revealed that photo-Fenton and photo-Fenton/Nb_2O_5 processes are more efficient than dark-Fenton process, that was most probably caused by the generation of additional HO• radicals in the two former processes. The optimum value of Fe^{2+} concentration for effective decolorization of aqueous RhB by photo-Fenton process also determined that was 50 mg L^{-1} with 99% decolorization of RhB within 2 min.

References

[1] M.F. Abdel-Messih, M.A. Ahmed, A.S. El-Sayed, Photocatalytic decolorization of Rhodamine B dye using novel mesoporous SnO_2–TiO_2 nano mixed oxides prepared by sol–gel method, J. Photochem. Photobiol., A 260 (2013) 1–8.

[2] L. Shi, L. Liang, J. Ma, Y. Meng, Sh. Zhong, F. Wang, J. Sun, Highly efficient visible light-driven Ag/AgBr/ZnO composite photocatalyst for degrading Rhodamine B, Ceram. Int. 40 (2014) 3495–3502.

[3] S.-M. Lam, J.-C. Sin, A.Z. Abdullah, A.R. Mohamed, Degradation of wastewaters containing organic dyes photocatalysed by zinc oxide: A review, Desalin. Water Treat. 41 (2012) 131–169.

[4] S.-A. Ong, L.-N. Ho, Y.-S. Wong, O.-M. Min, L.-S. Lai, S.-K. Khiew, V. Murali, Photocatalytic mineralization of azo dye Acid Orange 7 under solar light irradiation, Desalin. Water Treat. 48 (2012) 245–251.

[5] R.H. Souther, T.A. Alspaugh, Textile wastes-recovery and treatment, J. Water Pollut. Control Fed. 29 (1957) 804–809.

[6] A. Hamza, M.F. Halmoda, Multiprocess treatment of textile wastewater, Proc. 35th Purdue Industrial Waste Congress, West Lafayette, IN, 1980.

[7] J.P. Lorimer, T.J. Mason, M. Plattes, S.S. Phull, D.J. Walton, Degradation of dye effluent, Pure Appl. Chem. 12 (2001) 1957–1968.

[8] H. Farhadi, F. Hashemzadeh, R. Rahimi, A. Gaffarinejad, Surfactant-free hydrothermal synthesis of mesoporous niobia samples and their photoinduced decomposition of terephthalic acid (TPA), J. Cluster Sci. 25 (2014) 651–666.

[9] F. Hashemzadeh, R. Rahimi, A. Gaffarinejad, Influence of operational key parameters on the photocatalytic decolorization of rhodamine B dye using $Fe^{2+}/H_2O_2/Nb_2O_5$/UV system, Environ. Sci. Pollut. Res. 21 (2014) 5121–5131.

[10] F. Hashemzadeh, R. Rahimi, A. Ghaffarinejad, Mesoporous nanostructures of Nb_2O_5 obtained by an EISA route for the treatment of malachite green dye-contaminated aqueous solution under UV and visible light irradiation, Ceram. Int. 40 (2014) 9817–9829.

[11] D. Ollis, Kinetics of photocatalyzed film removal on self-cleaning surfaces: Simple configurations and useful models, Appl. Catal., B 99 (2010) 478–484.

[12] M.L. Marin, G. Hallett-Tapley, S. Impellizzeri, C. Fasciani, S. Simoncelli, J.C. Netto-Ferreira, T. Scaiano, Synthesis, acid properties and catalysis by niobium oxide nanostructured materials, Catal. Sci. Technol. (2014), doi:10.1039/C4CY00238E.

[13] J. Yan, G. Wu, N. Guan, L. Li, Nb_2O_5/TiO_2 heterojunctions: Synthesis strategy and photocatalytic activity, Appl. Catal., B 152–153 (2014) 280–288.

[14] M. Schmitt, M.A. Aegerter, Electrochromic properties of Nb2O5 and Nb2O5: X sol-gel coatings (X = Sn, Zr, Li, Ti, Mo), Proc. SPIE 3788, Switchable Materials and Flat Panel Displays, 3788 (1999) 93–102, SPIE Digital Library, Bellingham.

[15] R.A. Kadir, R. Abdul Rani, A.S. Zoolfakar, J.Z. Ou, M. Shafiei, W. Wlodarski, K. Kalantar-zadeh, Nb_2O_5 Schottky based ethanol vapour sensors: Effect of metallic catalysts, Sens. Actuators, B 202 (2014) 74–82.

[16] H. Szymanowski, O. Zabeida, J.E. Klemberg-Sapieha, L. Martinu, Optical properties and microstructure of plasma deposited Ta_2O_5 and Nb_2O_5 films, J. Vac. Sci. Technol. A 23 (2005) 241–247.
[17] Y. Zhao, C. Eley, J. Hu, J. S. Foord, L. Ye, H. He, S. C. E. Tsang, Shape-Dependent Acidity and Photocatalytic Activity of Nb_2O_5 Nanocrystals with an Active TT (001) Surface, Angew. Chem. Int. Ed. 51 (2012) 3846–3849.
[18] N.A. Dsouki, M.P. de Lima, R. Corazzini, T.M. Gáscon, L.A. Azzalis, V.B.C. Junqueira, D. Feder, F.L.A. Fonseca, Cytotoxic, hematologic and histologic effects of niobium pentoxide in Swiss mice, J. Mater. Sci.: Mater. Med. 25 (2014) 1301–1305.
[19] S.-K. Kim, E.-S. Kwon, T.-H. Kim, J. Moon, J. Kim, Effects of atmospheric Ti(III) reduction on Nb_2O_5-doped $Li_4Ti_5O_{12}$ anode materials for lithium ion batteries, Ceram. Int. 40 (2014) 8869–8874.
[20] J.G. Weissman, E.I. Ko, P. Wynblatt, J.M. Howe, High-resolution electron microscopy and image simulation of TT-,T-, and H-niobia and model silica-supported niobium surface oxides, Chem. Mater. 1 (1989) 187–193.
[21] S. Qi, R. Zuo, Y. Liu, Y. Wang, Synthesis and photocatalytic activity of electrospun niobium oxide nanofibers, Mater. Res. Bull. 48 (2013) 1213–1217.
[22] S. Ge, H. Jia, H. Zhao, Z. Zheng, L. Zhang, First observation of visible light photocatalytic activity of carbon modified Nb_2O_5 nanostructures, J. Mater. Chem. 20 (2010) 3052–3058.
[23] J.J. Pignatello, D. Liu, P. Huston, Evidence for an additional oxidant in the photoassisted Fenton reaction, Environ. Sci. Technol. 33 (1999) 1832–1839.
[24] L.G. Devi, K.E. Rajashekhar, K.S.A. Raju, S.G. Kumar, Influence of various aromatic derivatives on the advanced photo Fenton degradation of Amaranth dye, Desalination 270 (2011) 31–39.
[25] A.N. Soon, B.H. Hameed, Heterogeneous catalytic treatment of synthetic dyes in aqueous media using Fenton and photo-assisted Fenton process, Desalination 269 (2011) 1–16.
[26] C. Leon y Leon, J. Solar, V. Calemma, L. Radovic, Evidence for the protonation of basal plane sites on carbon, Carbon 30 (1992) 797–811.
[27] G. Newcombe, R. Hayes, M. Drikas, Granular activated carbon: Importance of surface properties in the adsorption of naturally occurring organics, Colloids Surf., A 78 (1993) 65–71.
[28] M. Liu, D. Xue, Amine-assisted route to fabricate $LiNbO_3$ particles with a tunable shape, J. Phys. Chem. C 112 (2008) 6346–6351.
[29] J. Lin, J. Lin, Y. Zhu, Controlled synthesis of the $ZnWO_4$ nanostructure and effects on the photocatalytic performance, Inorg. Chem. 46 (2007) 8372–8378.
[30] B.N. Patil, D.B. Naik, V.S. Shrivastava, Photocatalytic degradation of hazardous Ponceau-S dye from industrial wastewater using nanosized niobium pentoxide with carbon, Desalination 269 (2011) 276–283.
[31] X. Wang, G. Chen, C. Zhou, Y. Yu, G. Wang, N-doped Nb_2O_5 sensitized by carbon nitride polymer—Synthesis and high photocatalytic activity under visible light, Eur. J. Inorg. Chem. 2012 (2012) 1742–1749.
[32] Y. Huai, X. Hu, Z. Lin, Z. Deng, J. Suo, Preparation of nano-TiO_2/activated carbon composite and its electrochemical characteristics in non-aqueous electrolyte, Mater. Chem. Phys. 113 (2009) 962–966.
[33] J.-H. Sun, Y.-K. Wang, R.-X. Sun, S.-Y. Dong, Photodegradation of azo dye Congo Red from aqueous solution by the WO_3–TiO_2/activated carbon (AC) photocatalyst under the UV irradiation, Mater. Chem. Phys. 115 (2009) 303–308.
[34] J. Rivera-Utrilla, I. Bautista-Toledo, M.A. Ferro-García, C. Moreno-Castilla, Activated carbon surface modifications by adsorption of bacteria and their effect on aqueous lead adsorption, J. Chem. Technol. Biotechnol. 76 (2001) 1209–1215.
[35] A.G.S. Prado, L.L. Costa, Photocatalytic decouloration of malachite green dye by application of TiO_2 nanotubes, J. Hazard. Mater. 169 (2009) 297–301.
[36] S. Tangestaninejad, M. Moghadam, V. Mirkhani, I. Mohammadpoor-Baltork, H. Salavati, Sonochemical and visible light induced photochemical and sonophotochemical degradation of dyes catalyzed by recoverable vanadium-containing polyphosphomolybdate immobilized on TiO_2 nanoparticles, Ultrason. Sonochem. 15 (2008) 815–822.
[37] N. Shimizu, C. Ogino, M.F. Dadjour, T. Murata, Sonocatalytic degradation of methylene blue with TiO_2 pellets in water, Ultrason. Sonochem. 14 (2007) 184–190.
[38] Q. Wang, M. Zhang, C. Chen, W. Ma, J. Zhao, Photocatalytic aerobic oxidation of alcohols on TiO_2: The acceleration effect of a Brønsted acid, Angew. Chem. Int. Ed. 49 (2010) 7976–7979.
[39] S. Merouani, O. Hamdaoui, F. Saoudi, M. Chiha, Sonochemical degradation of Rhodamine B in aqueous phase: Effects of additives, Chem. Eng. J. 158 (2010) 550–557.
[40] S. Malato, J. Blanco, C. Richter, B. Braun, M.I. Maldonado, Enhancement of the rate of solar photocatalytic mineralization of organic pollutants by inorganic oxidizing species, Appl. Catal., B 17 (1998) 347–356.
[41] G.R. Helz, R.G. Zepp, D.G. Crosby, Aquatic and Surface Photochemistry, Lewis Publishers, Boca Raton, 1994.
[42] M. Muruganandham, M. Swaminathan, Solar photocatalytic degradation of a reactive azo dye in TiO_2-suspension, Sol. Energy Mater. Sol. Cells 81 (2004) 439–457.
[43] I.K. Konstantinou, T.A. Albanis, TiO_2-assisted photocatalytic degradation of azo dyes in aqueous solution: Kinetic and mechanistic investigations, Appl. Catal., B 49 (2004) 1–14.
[44] C. Walling, Fenton's reagent revisited, Acc. Chem. Res. 8 (1975) 125–131.
[45] C.L. Hsueh, Y.H. Huang, C.C. Wang, C.Y. Chen, Degradation of azo dyes using low iron concentration of Fenton and Fenton-like system, Chemosphere 58 (2005) 1409–1414.